Enhanced optical properties due to indium incorporation in zinc oxide nanowires

S. Farid,[1] S. Mukherjee,[1] K. Sarkar,[1] M. Mazouchi,[1] M. A. Stroscio,[1,2,3] and M. Dutta[1,2,a)]
[1]*Department of Electrical and Computer Engineering, University of Illinois at Chicago, Chicago, Illinois 60607, USA*
[2]*Department of Physics, University of Illinois at Chicago, Chicago, Illinois 60607, USA*
[3]*Department of Bioengineering, University of Illinois at Chicago, Chicago, Illinois 60607, USA*

(Received 12 November 2015; accepted 20 December 2015; published online 11 January 2016)

Indium-doped zinc oxide nanowires grown by vapor-liquid-solid technique with 1.6 at. % indium content show intense room temperature photoluminescence (PL) that is red shifted to 20 meV from band edge. We report on a combination of nanowires and nanobelts-like structures with enhanced optical properties after indium doping. The near band edge emission shift gives an estimate for the carrier density as high as $5.5 \times 10^{19}\,cm^{-3}$ for doped nanowires according to Mott's critical density theory. Quenching of the visible green peak is seen for doped nanostructures indicating lesser oxygen vacancies and improved quality. PL and transmission electron microscopy measurements confirm indium doping into the ZnO lattice, whereas temperature dependent PL data give an estimation of the donor and acceptor binding energies that agrees well with indium doped nanowires. This provides a non-destructive technique to estimate doping for 1D structures as compared to the traditional FET approach. Furthermore, these indium doped nanowires can be a potential candidate for transparent conducting oxides applications and spintronic devices with controlled growth mechanism. © *2016 AIP Publishing LLC*. [http://dx.doi.org/10.1063/1.4939454]

It is well known that doping in zinc oxide with specific dopants can enhance its electrical and optical properties.[1–3] Although *p*-type doping in ZnO still remains a challenge, it is equally important to achieve *n*-type doping in ZnO with controllable carrier concentrations, ease of fabrication, and high crystallinity that can be used for optoelectronic and spintronic applications.[4] Various group III elements such as Ga, Al and transition metals such as Fe and Mn along with rare earth elements such as Er and Eu have been doped into ZnO thin films for variety of applications.[5,6] However, reports on one-dimensional indium doped ZnO nanowires still remain rare, and the role of indium as a luminescence activator and an *n* compensator is rarely explored. Some researchers have explored aluminum, (Al), as a dopant for ZnO in detail.[7,8] This is because the ionic radius of Al is smaller than that of Ga and In. However, considering the thermodynamic data, it is revealed that the free energy for the formation of Al_2O_3 is lower as compared to zinc oxide, suggesting that aluminum oxide has a very high reactivity with oxygen.[9] In this scenario, indium possesses greater resistivity to oxidation along with less reactivity as compared to *Al* making it an attractive dopant for n-type ZnO. Jie *et al.*,[10] Xu *et al.*,[11] and few other researchers[12,13] have reported indium doped ZnO nanobelts (NBs) using thermal evaporation route, but most of them reported structural or room temperature photoluminescence (PL) studies. There are only a few reports on temperature dependent PL studies on indium doped ZnO nanowires.[14–16] Amongst them, Chen *et al.*[14] prepared ZnO:In nanorods by sol-gel technique, Morales *et al.*[15] synthesized indium doped nanostructures using chemical synthesis technique, whereas Liu *et al.*[16] reported temperature dependent studies of In doped ZnO nanowires grown on sapphire substrates. In this study, we have used a vapor-liquid-solid (VLS) growth technique to dope 1D ZnO nanostructures on silicon substrates for better control, optimization, and cheaper solution and explored optical and structural properties. Along with this, we have also performed a deep defect state analysis of doped ZnO nanowires (NWs) using temperature dependent PL studies since that can provide useful information on the dissociation processes due to the impurity bound excitons. We have also reported enhanced optical properties from In doped ZnO NWs (IZO) owing it to be a good candidate for future spintronic devices,[16] transparent conducting oxide materials,[17] photodetectors,[18] and gas sensors applications.[19,20]

ZnO and In_2O_3 powders with purities of 99.99% and 99.998%, respectively, are used as precursors. Gold film with nominal thickness of ~4 nm is deposited on Si substrate. A mixture of ZnO and graphite at a weight ratio of 1:1 is mixed together and is used as a source to prepare undoped ZnO NWs. For growth of IZO nanowires, In_2O_3 powder (99.999% pure) is added as a reaction source to ZnO and graphite mixture with 3% weight ratio, and the whole mixture is mixed together on a centrifugal mixture at 1000 rpm for uniform distribution of powder. Average atomic concentration for Indium in ZnO is estimated using energy dispersive x-ray detector (EDX) analysis. Choice of percentage selection for indium oxide is based on our representative result; however, effects on the optical properties on percentage variations of indium oxide will be presented in subsequent archival studies. The mixture was then placed in the ceramic boat and placed in the middle of the 2 in. diameter quartz tube in the furnace. The boat was positioned in the

a)Author to whom correspondence should be addressed. Electronic mail: dutta@uic.edu

center of the quartz furnace tube, and the Si substrate with ⟨100⟩ crystal orientation coated with 4 nm gold was placed 2 cm downstream from the mixed powders. The growth was carried out at 910 °C for ∼40 min duration at 150 sccm at a constant argon flow as a carrier gas. Structure was characterized using a variable-pressure Hitachi S-3000N scanning electron microscope (SEM). Optical properties are investigated using photoluminescence spectroscopy at room temperature with a 325 nm He-Cd laser using an Acton 2500i spectrometer, while low temperature PL investigation is done in a closed cycle helium cryostat. Transmission electron microscopy (TEM) of the nanostructures was carried out using a JEOL JEM 3010 electron microscope.

Figure 1(a) shows a SEM image of as-grown ZnO NWs. It can be seen that the Si substrate is covered with tangled ZnO nanowires with diameters of 50–100 nm and lengths up to 10–50 μm. In case of IZO samples, along with nanowires, we observe a few NBs dispersing in nanowires. Figs. 1(b)–1(d) shows indium doped NWs and NBs at different magnifications. Diameters of doped NWs are in the range of 100–200 nm, whereas NBs reveal widths up to 500 nm and thickness ∼20 nm. Some of the NBs appear to be smooth along their lengths, while some shows a zig zag structure.

For obtaining more insight into individual nanowires and nanobelts of doped ZnO structures, HRTEM, selected area electron diffraction (SAED), and EDX measurements have been carried, and the results are shown in Figs. 2(a)–2(f). We did not observe any lattice distortions, stacking faults, or evidence of amorphous outer layer from the TEM profile. For doped NWs, the hexagonal lattice fringes are spaced ∼2.94 ± 0.01 Å apart (Fig. 2(a)) which is slightly greater than the as-grown ZnO lattice spacing of

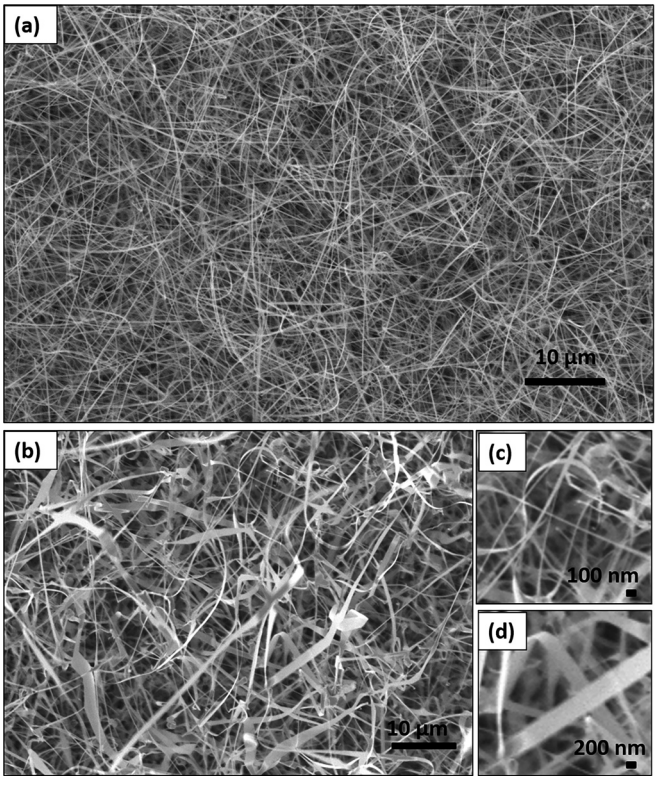

FIG. 1. SEM image of (a) ZnO NWs; (b) IZO NWs and NBs; (c) IZO NWs with ∼50–100 nm diameter; and (d) IZO NBs with ∼500 nm diameter.

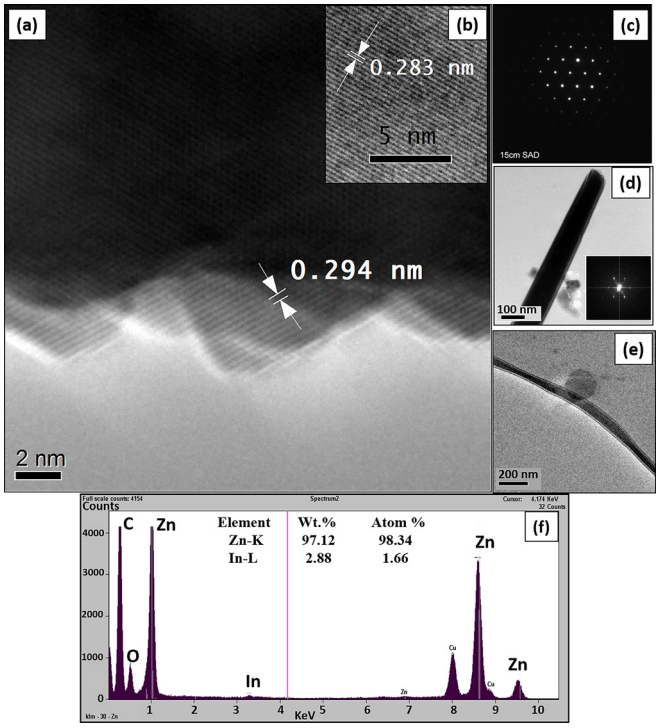

FIG. 2. (a) TEM image of IZO nanowires showing lattice spacing of 0.294 nm; (b) TEM image of undoped ZnO nanowires with 0.283 nm lattice spacing; (c) SAED pattern for indium doped zinc oxide nanostructures; (d) TEM image of 100 nm IZO NW (inset shows Fast Fourier transform measurements for IZO nanostructures); (e) TEM image of a non-uniform IZO NB; and (f) EDX profile for obtaining elemental composition of IZO nanostructures.

∼2.83 ± 0.01 Å (Fig. 2(b)). A possible reason for the increase in *d* spacing could be doping related as indium ionic radius is higher than ZnO that accounts for variation in lattice spacing.[13] This variation in *d* spacing could not be explained by the TEM measurement's error bar, which is less than 0.01 Å. SAED measurement is performed to confirm the crystal structure of doped NWs (Fig. 2(c)). Hexagonal diffraction pattern reveals wurtzite structure with single crystalline properties. From the SAED pattern, we can also reveal that the doped NWs are grown along [0001] direction. EDX measurements have also been made on many doped ZnO structures, and In peak is found in most of them (Fig. 2(f)). The atomic percentage estimated from EDX for IZO nanowires is ∼1.6%. We also observed some of the NBs seems to be non-uniform through its length as shown in Fig. 2(d).

In order to investigate further into the possible reasons for the structural change from the thinner NWs to larger diameter of nanowires and nanobelts with increasing the concentration of Indium, an understanding of the possible growth process is necessary. An important factor to consider is the surface energy that affects the growth of nanowires and determines the necessary controlled nucleation growth conditions. For our case, indium content is much lower than the zinc content, and zinc and indium are transported to the substrate at elevated temperature. These vapors further react with Au and give rise to a Au-In-Zn ternary phase. Since the surface free energy is defined as the free excess surface energy per unit area for a particular crystal geometry and face, a certain strain resulting from ternary Au-In-Zn phase

gives rise to variations of surface free energy that disturbs the equilibrium crystal shape and modifies the nucleation behavior of zinc oxide resulting in nanobelts formation. Similar observation of a ternary Au-Zn-In phase has been observed by Fan *et al.*[21] As for the non-uniform belts, it might be due to some thermal instability or strain during the liquid-solid interface phase for the VLS growth mechanism that can also explain the possible cause for the wider diameters of the nanowires for the *In* doped ZnO structures.

Figure 3(a) shows the PL spectra of ZnO and IZO NWs at room temperature. As it can be seen that the undoped ZnO NWs shows weak near-band-edge (NBE) emission at 3.25 eV (381.5 nm), while broad strong visible emission (VE) at 2 .45 eV due to deep level defect states often related to oxygen vacancies is seen which has been extensively studied in the past decade.[22,23] Interestingly, after In doping, we see a strong enhancement in NBE peak which is almost 20 times stronger than pure ZnO nanowires while, VE is decreased significantly owing to change in the growth kinetics due to In supply which helps to reduce the number of defects states resulting in improved crystal quality. Along with enhancement in NBE peak, we also observe a red shift in energy to 3.23 eV (383.9 nm) as observed by other researchers[24,25] as well due to In doping in GaN and GaAs based thin-films and nanostructures. Such a red shift could be a result of potential fluctuation induced by the introduction of impurity atoms resulting in optical band gap narrowing of nanostructures.[13] Also according to Motts critical density theory, band gap tends to increase if the impurity is kept under Motts critical density limit. After the conduction band is already filled and more impurity atoms are added to the semiconductor, merging of conduction and donor band levels happens and the band gap tends to decrease.[26] Based on the calculations presented by Kim and Park,[27] we estimate the carrier concentration for our indium doped nanowires to be $\sim 5.5 \times 10^{19}\,\mathrm{cm}^{-3}$. The reason for an enhanced NBE peak could be explained in two different ways; either this effect is due to the lower concentrations of surface states in thicker doped NWs diameters that can be explained by the lesser surface to volume ratio as compared to their undoped thinner counterparts or it is also expected that the formation of bound electrons in the indium doped samples is enhanced that resulted in strong NBE peak.[28] Morales *et al.*[15] also observed 10 times enhancement from indium doped samples which is suggested to be a transition from a shallow defect state and a deep level. We explored this effect in detail at low temperature PL spectra and found a clear difference in the PL spectra of doped and undoped nanowires at 20 K as shown in Fig. 3(b). For undoped ZnO NWs, the dominant peak is seen at 3.351 eV attributed to the bound exciton emission peak, likely originating from D^oX. A small peak at the high energy side of D^oX (3.358 eV) is contributed to the surface bound excitons (SX) that completely disappears at

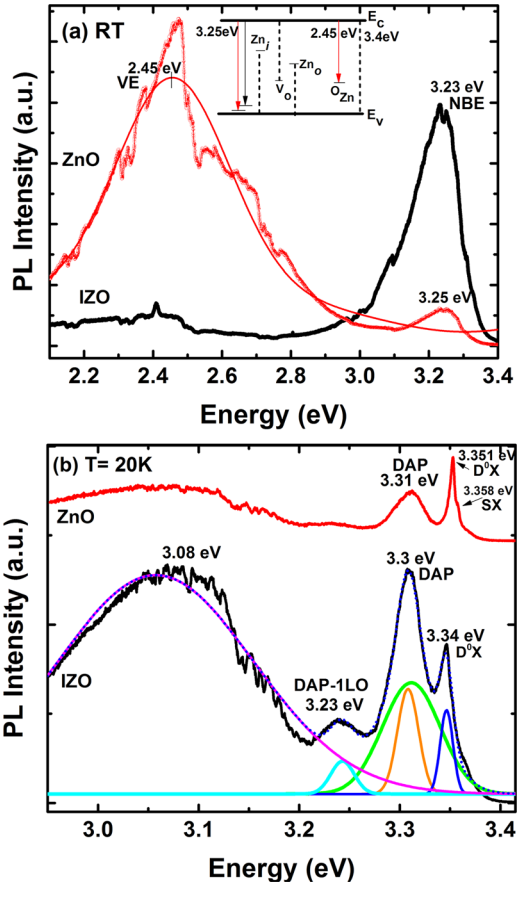

FIG. 3. (a) Room temperature (RT) PL spectra for the ZnO and IZO NWS; ZnO VE is fitted with Gaussian fit to account for peak variances; Inset indicates schematic of possible transitions from ZnO structures, (NBE emission at 3.25 eV, oxygen antisite (O_{Zn}), oxygen vacancies (V_o) or Zinc vacancies (Zn_o), Zinc antisites in the oxide (Zn_i)); (b) PL spectra at 20 K for ZnO and IZO NWs with Gaussian peak fits presented for IZO nanowires.

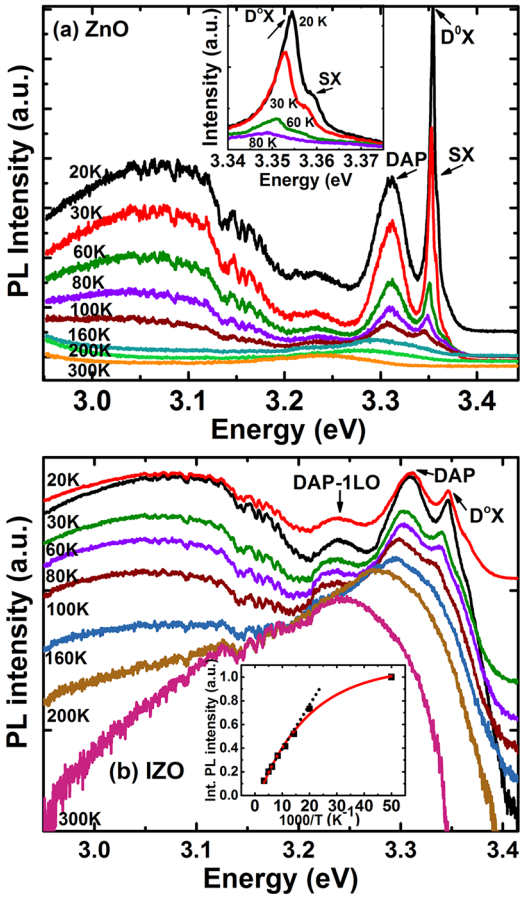

FIG. 4. (a) Temperature dependent PL spectra of (a) ZnO; (b) IZO NWs. (The inset shows temperature dependence of DAP on PL intensities.)

higher temperatures (shown later in Fig. 4(a)). We also observe an emission at 3.31 eV which is attributed to donor-acceptor pair (DAP) recombination and matches well with others in literature.[29,30] Another weak broad band at 3.07 eV is seen which becomes significant for In doped NWs. We did not see this peak for doped nanowires in previous efforts[14–16] and its origin is still under investigation. This peak may be associated with the phonon replicas of free excitons in case it falls into the LO phonon replicas of ZnO (~72 meV) which is hard to extract from our results due to the broadened and smeared nature of the peak or purely related to In doping effect. After In doping, the PL spectra at 20 K indicate some different features compared to pure ZnO NWs. These PL spectra can be well fitted by five Gaussian peaks as shown in Fig. 3(b). We found that D^oX happens at 3.34 eV instead of 3.357 eV which is generally documented for lightly doped indium films indicating that we have achieved heavily doped ZnO nanowires with 1.6 at. % indium content.[14] A similar observation is seen by He *et al.*[29] who confirmed 3.346 eV emission obtained for 1.4 at. % indium doping due to exciton bound to In site confirming that In atoms have been doped into the ZnO lattice and substitute the Zn sites. We did not observe any SX emission for doped NWs. Intensity of DAP also increases with a small shift towards the lower energy side which is believed to be due to increased bound exciton formation due to In doping.[15,31] Visible emission peaks due to oxygen, zinc vacancies, and zinc interstitial defects are not shown here. We also observe another emission band at 3.23 eV which was not seen for undoped NWs. We assign this peak to be LO phonon replica of DAP recombination as it has an energy ~70 meV lower than DAP.[31] In order to further investigate and verify our assignments, temperature dependent PL experiments were carried out.

Figures 4(a) and 4(b) show temperature dependent PL of ZnO and IZO, respectively. For ZnO NWs (Fig. 4(a)), the intensity of D^oX and DAP decreased significantly as the temperature increases and a shift in lower energy side is observed. The SX emission disappears completely at >30 K temperature as shown in the inset of Fig. 4(a) confirming our assignment related to surface excitons. Attenuation of D^oX emission and its merging into DAP seems reasonable as the free excitons thermalize and cannot be seen at higher temperatures. Since the curves at each temperature have been offset with respect to each other for more visibility, the emissions at higher temperature appear to be less visible. For In doped NWs, we did not see any SX emission at all which agrees with Liu *et al.*[14] With increasing temperatures, the peaks overlap with each other and ultimately shift and merge to a broader peak possibly due to the phonon scattering effects as the temperature reaches to higher orders. Taking a close look at DAP, it is seen that it is broader as compared to D^oX line. We did a quantitative evaluation of the temperature dependence of DAP transition intensities as presented in the inset of Fig. 4(b). The dotted squares presents experimental data, and curve is fitted by well known Arrhenius equation using the following formula:[32,33]

$$I(T) = \frac{I_0}{1 + A_1 \exp\left(-\frac{E_1}{K_B T}\right) + A_2 \exp\left(-\frac{E_2}{K_B T}\right)}. \quad (1)$$

Here, $I(T)$ and I_0 are the PL intensities at temperature T and 20 K, respectively; E_i is the activation energy, K_B is the Boltzmann constant, and A_i is the constant. By making A_2 zero and considering there is only one quenching channel contributing to decrease in intensity of DAP with temperature, we are not able to obtain the best fit curve for the data. By using a two channel fit and considering both A_1 and A_2 constants, we found E_1 and E_2 to be 32 meV and 9 meV, respectively. We suggest that the small activation energy corresponds to the effective ionization energy for the donors, whereas acceptor like states is activated at 32 meV. Recent experimental and theoretical results have shown that for *n* type doped ZnO, acceptor like complexes can act as a compensating center.[29,34,35] This allows us to conclude that the direct transitions between the tails of valence and conductions bands account for the remarkable PL intensity for indium doped IZO nanowires.

In summary, we have achieved an intense NBE peak in ZnO NWs after doping it with 1.6 at. % In content. SEM images reveal the formation of NWs and NBs after doping with indium oxide with thicker diameter and larger width to thickness ratios. TEM and SAED measurements confirm indium doping into ZnO lattice and resulting structure has high crystalline quality. We also observed a reduction in VE, indicating fewer oxygen vacancies and improved optical properties for doped NWs. The PL shows a redshift of peak energy for doped NWs, and the carrier concentration is estimated according to Mott's critical density theory to be $5.5 \times 10^{19}\,cm^{-3}$. Emission peak at 3.34 eV for 1.6 at. % indium doped nanowires is found to be due to exciton bound to In site confirming that In atoms have been doped into the ZnO lattice. Low temperature PL spectra indicate that D^oX merges and DAP recombination dominates at higher temperatures for indium doped NWs. Thermal quenching of PL at higher temperatures reveals activation energy for the donor and acceptor to be 32 meV and 9 meV, respectively. Our works provide a non-destructive way for estimating doping using PL measurements and suggest that In doping in ZnO NWs can be used for advancements in optoelectronics and spintronic devices.

This work was partially supported by Grant No. FA9550-15-1-0493 from the Air Force Office of Scientific Research. Author S.F. would like to thank Fulbright and IIE for support of this work. We would also like to thank Dr. Alan Nicholls from Research Resource Center, University of Illinois at Chicago for his insight and useful discussions on our TEM results. This work made use of instruments in the Electron Microscopy Service (Research Resources Center, UIC).

[1]C. X. Xu, X. W. Sun, and B. J. Chen, Appl. Phys. Lett. **84**, 1540 (2004).
[2]R. Könenkamp, R. C. Word, and M. Godinez, Nano Lett. **5**, 2005 (2005).
[3]F. X. Xiu, Z. Yang, L. J. Mandalapu, D. T. Zhao, J. L. Liu, and W. P. Beyermann, Appl. Phys. Lett. **87**, 152101 (2005).
[4]S. Farid, M. Purahmad, M. A. Stroscio, and M. Dutta, in *2012 15th International Workshop on Computational Electronics (IWCE)* (IEEE, 2012), pp. 1–3.
[5]Q. H. Li, D. Zhu, W. Liu, Y. Liu, and X. C. Ma, Appl. Surf. Sci. **254**, 2922 (2008).
[6]X. Yu, J. Ma, F. Ji, Y. Wang, C. Cheng, and H. Ma, Appl. Surf. Sci. **245**, 310 (2005).

[7]Y. Liu and J. Lian, Appl. Surf. Sci. **253**, 3727 (2007).
[8]X. Jiang, F. L. Wong, M. K. Fung, and S. T. Lee, Appl. Phys. Lett. **83**, 1875 (2003).
[9]G. Singh, S. B. Shrivastava, D. Jain, S. Pandya, T. Shripathi, and V. Ganesan, Bull. Mater. Sci. **33**, 581 (2010).
[10]J. Jie, G. Wang, X. Han, Q. Yu, Y. Liao, G. Li, and J. G. Hou, Chem. Phys. Lett. **387**, 466 (2004).
[11]L. Xu, Y. Su, Y. Chen, H. Xiao, L. A. Zhu, Q. Zhou, and S. Li, J. Phys. Chem. B **110**, 6637 (2006).
[12]B. Aleman, P. Fernandez, and J. Piqueras, Appl. Phys. Lett. **95**, 013111 (2009).
[13]J. Jie, G. Wang, X. Han, and J. G. Hou, J. Phys. Chem. B **108**, 17027 (2004).
[14]Y. W. Chen, Y. C. Liu, S. X. Lu, C. S. Xu, C. L. Shao, C. Wang, J. Y. Zhang, Y. M. Lu, D. Z. Shen, and X. W. Fan, J. Chem. Phys. **123**, 134701 (2005).
[15]A. E. Morales, R. Aceves, U. Pal, and J. Z. Zhang, J. Nanosci. Nanotechnol. **8**, 6538 (2008).
[16]K. W. Liu, M. Sakurai, and M. Aono, J. Appl. Phys. **108**, 043516 (2010).
[17]K. Ellmer, A. Klein, and B. Rech, *Transparent Conductive Zinc Oxide: Basics and Applications in Thin Film Solar Cells* (Springer Science & Business Media, 2007), Vol. 104.
[18]T. Zhai, X. Fang, M. Liao, X. Xu, H. Zeng, B. Yoshio, and D. Golberg, Sensors **9**, 6504 (2009).
[19]E. Comini, Anal. Chim. Acta **568**, 28 (2006).
[20]K. Xu, M. Purahmad, K. Brenneman, X. Meshik, S. Farid, S. Poduri, P. Pratap, J. Abell, Y. Zhao, B. Nichols, E. Zakar, M. Stroscio, and M. Dutta, "Design and applications of nanomaterial-based and biomolecule-based nanodevices and nanosensors," in *Design and Applications of Nanomaterials for Sensors* (Springer, Netherlands, 2014), p. 61–97.
[21]H. J. Fan, B. Fuhrmann, R. Scholz, C. Himcinschi, A. Berger, H. Leipner, A. Dadgar, A. Krost, S. Christiansen, U. Gösele, and M. Zacharias, Nanotechnology **17**, S231 (2006).
[22]B. D. Yao, Y. F. Chan, and N. Wang, Appl. Phys. Lett. **81**, 757 (2002).
[23]Y. Li, G. W. Meng, L. D. Zhang, and F. Phillipp, Appl. Phys. Lett. **76**, 2011 (2000).
[24]H. Kumano, K. Hoshi, S. Tanaka, I. Suemune, X. Shen, P. Riblet, P. Ramvall, and Y. Aoyagi, Appl. Phys. Lett. **75**, 2879 (1999).
[25]Y. Kim, H. J. Joyce, Q. Gao, H. H. Tan, C. Jagadish, M. Paladugu, J. Zou, and A. A. Suvorova, Nano Lett. **6**, 599 (2006).
[26]B. E. Sernelius, K. F. Berggren, Z. C. Jin, I. Hamberg, and C. G. Granqvist, Phys. Rev. B **37**, 10244 (1988).
[27]K. J. Kim and Y. R. Park, Appl. Phys. Lett. **78**, 475 (2001).
[28]A. Kar, M. A. Stroscio, M. Meyyappan, D. J. Gosztola, G. P. Wiederrecht, and M. Dutta, Nanotechnology **22**, 285709 (2011).
[29]H. P. He, Z. Wang, H. F. Duan, and Z. Z. Ye, Phys. Chem. Chem. Phys. **17**, 17552 (2015).
[30]Q. Jijun, X. Li, W. He, S. Park, H. Kim, Y. Hwang, J. Lee, and Y. Kim, Nanotechnology **20**, 155603 (2009).
[31]L. Duan, B. Lin, W. Zhang, S. Zhong, and Z. Fu, Appl. Phys. Lett. **88**, 232110 (2006).
[32]X. C. Shan, Z. Liu, and S. K. Hark, Appl. Phys. Lett. **92**, 73103 (2008).
[33]S. Farid, S. Mukherjee, H. Jung, M. A. Stroscio, and M. Dutta, Mater. Res. Express **2**, 025007 (2015).
[34]J. E. Stehr, K. M. Johansen, T. S. Bjørheim, L. Vines, B. G. Svensson, W. M. Chen, and I. A. Buyanova, Phys. Rev. Appl. **2**, 021001 (2014).
[35]E. Iliopoulos, D. Doppalapudi, H. M. Ng, and T. D. Moustakas, Appl. Phys. Lett. **73**, 375 (1998).